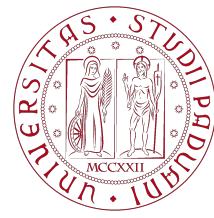


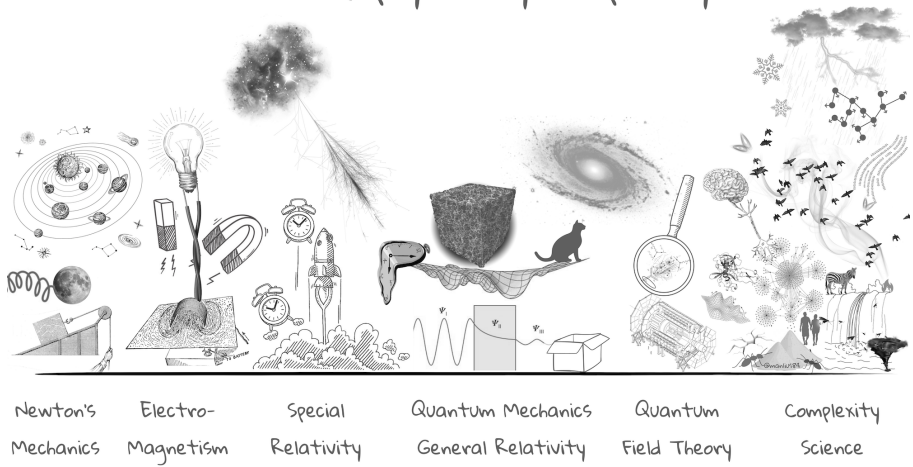
# Final Report

Physics of Complex Networks: Structure and Dynamics



UNIVERSITÀ  
DEGLI STUDI  
DI PADOVA

Areas of physics by complexity



## Project # 9

Jelin Raphael Akkara  
Davide Checchia  
Kiamehr Javid  
Joan Verguizas I Moliner  
Giuseppe Bevilacqua

Team name: Sociophysics

Last update: September 9, 2023

# Contents

---

|  |           |
|--|-----------|
| <b>1 Voter model</b>                                   | <b>1</b>  |
| 1.1 Introduction . . . . .                             | 1         |
| 1.2 Voter model basics . . . . .                       | 1         |
| 1.3 Parameters and topologies . . . . .                | 2         |
| 1.4 Results . . . . .                                  | 4         |
| 1.4.1 Dimensionality . . . . .                         | 4         |
| 1.4.2 Degree distribution: SSF vs SW . . . . .         | 4         |
| 1.4.3 Node-update vs Edge-update . . . . .             | 6         |
| <b>2 Axelrod model for dissemination of culture</b>    | <b>7</b>  |
| 2.1 Introduction . . . . .                             | 7         |
| 2.2 Model Description . . . . .                        | 7         |
| 2.3 Model Analysis . . . . .                           | 8         |
| 2.3.1 Variation of $F$ and $q$ . . . . .               | 8         |
| 2.3.2 Variation of $R$ . . . . .                       | 8         |
| 2.3.3 Topological traits . . . . .                     | 8         |
| 2.4 Phase transition and active bonds . . . . .        | 9         |
| 2.5 Real-world data . . . . .                          | 10        |
| <b>3 Language Competition Dynamics</b>                 | <b>14</b> |
| 3.1 Introduction . . . . .                             | 14        |
| 3.2 Model Description . . . . .                        | 14        |
| 3.3 Model Analysis . . . . .                           | 15        |
| 3.3.1 Number of Nodes N . . . . .                      | 16        |
| 3.3.2 Changing the Topology . . . . .                  | 16        |
| 3.3.3 Prestige and Volatility . . . . .                | 16        |
| 3.4 Modelling the Dynamics of Language Death . . . . . | 17        |
| <b>4 Bibliography</b>                                  | <b>22</b> |

# 1 | Voter model

---

**Task leader(s):** Kiamehr Javid, Jelin Raphael Akkara

## 1.1 | Introduction

---

Sociophysics, in a nutshell, centers on the utilization of physics-inspired models to conduct analysis on social phenomena. One of the most well-known models when dealing with binary subjects is the Voter model. Akin to its the Ising model, it deals with the ordering of a complex network through various dynamics. This report covers the basics and relevant definitions to the voter model, the role of topology, and provide simulations comparing update rules.

There are other notable dynamics such as noisy voter model or q-voter model which will not be covered in this report. The noisy voter model includes spontaneous opinion flips and in the q-voter model each node is influenced by its qth order neighborhood.

## 1.2 | Voter model basics

---

Given a graph G with N vertices and m edges, a binary opinion  $\sigma_i$  is assigned to each node i. We have:

$$\sigma_i \in \{-1, 1\}$$

Ordering is quantified with interface density denoted by  $\rho$  which is simply the fraction of edges connecting disagreeing nodes  $\sigma_i\sigma_j = -1$

$$\rho = \frac{\sum_{i=1}^N \sum_{j \in \mathcal{N}_i} \frac{1-\sigma_i\sigma_j}{2}}{\sum_{i=1}^N k_i}$$

A time-step in the voter dynamics corresponds to performing the elementary update rule N times such that the nodes are updated once on average. A time-step can be synchronous or asynchronous. In the former case, a frozen image of the network at time t is used as reference for updating the opinions while in the latter we update one node at a time.

The standard classical update rule is the node-update in which a random node takes the opinion of one of its randomly selected neighbors. Edge-update rule samples



Figure 1.1: 2D lattice Evolution subject to node-update dynamics

an edge and assigns a random opinion to both ends of the edge if they disagree and leaves them unchanged otherwise.

The behavior of the interface density  $\langle \rho \rangle$  carries interesting information. The mean value on  $\rho$  is carried out over the ensemble of networks with similar properties.

$\langle \rho \rangle = 0$  corresponds to the so called absorbing states of global consensus where every node has the same opinion.  $\langle \rho \rangle$  behaves differently in different topologies. a few of well known behaviors are listed below [9].

In case of lattices with dimensionality  $d \leq 2$ , the system shows unbounded growth of spatial domains this behavior is regarded as ordering. Fig 1.1 shows a 50 by 50 lattice at different stages. Conversely, in networks of higher dimensionality the system does not order, meaning that finite sized domains form quickly. This translates to a quick transition of  $\langle \rho \rangle$  from the initial value to a plateau value  $\langle \xi \rangle$  around which the average interface density fluctuates.  $l = \xi^{-1}$  is an estimate for the size of the mentioned domains. The finite sized fluctuations can then lead  $\langle \rho \rangle$  to an exponential decay to the absorbing states

$$\langle \rho \rangle \propto \xi e^{\frac{-t}{\tau}}$$

where  $\tau$  is the lifetime of the metastable state.

### 1.3 | Parameters and topologies

The structured scale-free network is an effectively one dimensional network with a scale free degree distribution [8]. This lets us compare the role of degree distribution while

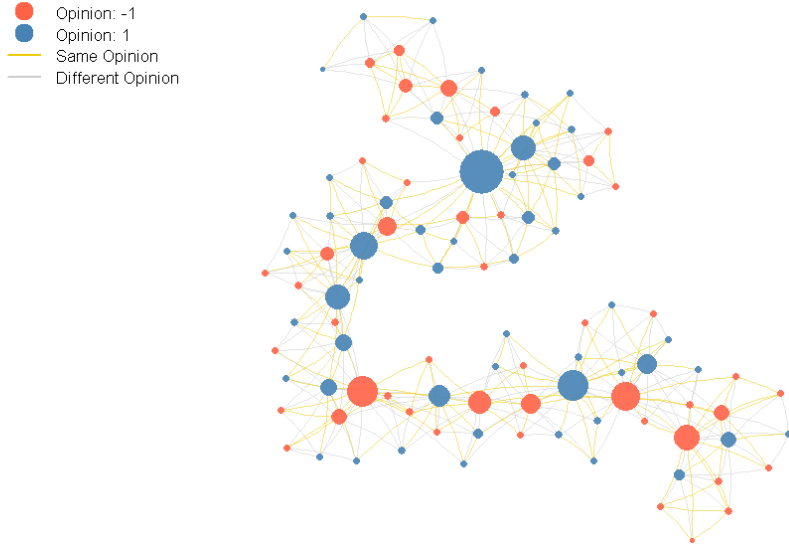


Figure 1.2: Structured Scale Free Network

keeping the dimensionality fixed. The network is grown via the node deactivation algorithm 1.2.

We will use the WS small world network with the same average degree  $\langle k \rangle$  as the network for comparison with the heterogeneous SSF. Small world networks will serve as the ensemble with homogeneous degree distribution.

The regular rewiring parameter  $p$  used for SW networks, can also be used on the SSF networks. Increasing  $p$  keeps the degree distribution and provides us a smooth transition from  $d = 1$  to infinite dimensionality by introducing a disorder to the system.

At the limit  $p = 1$ , SSF will behave as a random scale free network (RSF) and the SW turns into a random network (RN) with a fixed node degree.

- By changing the heterogeneity we will check the role of **degree distribution**
- **Dimensionality** can be loosely estimated as follows [12]: Let  $\mathcal{N}(v, k)$  be the number of nodes in the  $k$ -hop neighborhood of node  $v$ .

The scaling factor of  $k$  with  $\mathcal{N}(k)$  can be regarded as the dimension of a complex network where:

$$\mathcal{N}(k) = \frac{\sum_{v=1}^N \mathcal{N}(v, k)}{N}.$$

Super polynomial scaling of  $k$  can be viewed as  $d = \infty$ .

## 1.4 | Results

In this section we aim to replicate a number of previously found results for the node-update rule and compare them with the edge-update rule.

### 1.4.1 Dimensionality

Instead of estimating the dimensionality for each ensemble, the disorder parameter  $p$  acts as a tool for tuning the effective dimensionality. Increasing the disorder is supposed to shrink the size of communities in the meta-stable state and these smaller communities cause a less abrupt drop in  $\langle \rho \rangle$ . In other words,  $\xi$  increases and  $\tau$  decreases with disorder. This behavior is seen in both SW and SSF networks Fig. 1.3.

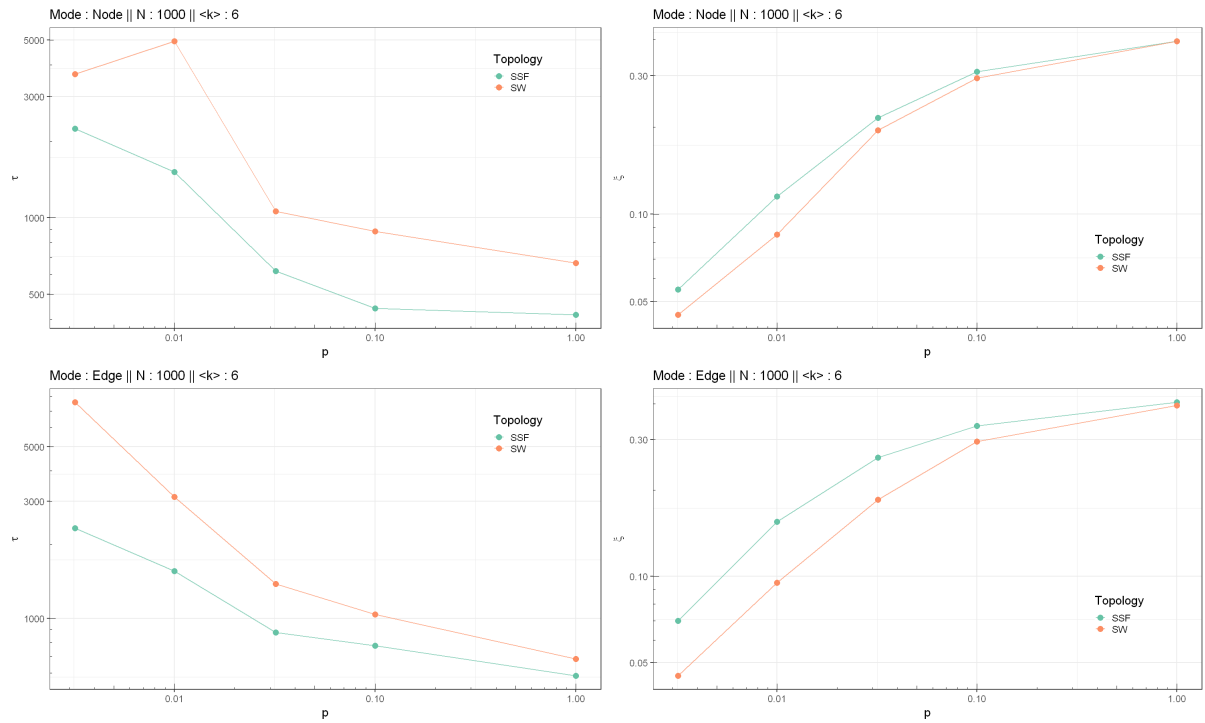


Figure 1.3: Variation of lifetime and plateau height with respect to disorder averaged over 32 realizations

Compared to the node-update rule, edge-update results in slightly higher values for both the plateau height and the lifetime in case of the SSF networks. However, the general behavior of the average interface density by varying disorder is not accurately distinguishable from the node-update dynamics in this attempt. Fig 1.4. This brings up the dependence of  $\langle \rho \rangle$  to the update-rule in a heterogeneous degree distribution.

### 1.4.2 Degree distribution: SSF vs SW

As expected for the effectively one dimensional networks using node-update,  $\langle \rho \rangle \propto t^{-1/2}$  and the SSF is almost always at a slightly higher interface density compared to the  $d = 1$  network. The power law is evident from the straight line in the log-log plot before the late stage exponential decay 1.5. The edge-update rule interestingly shows the

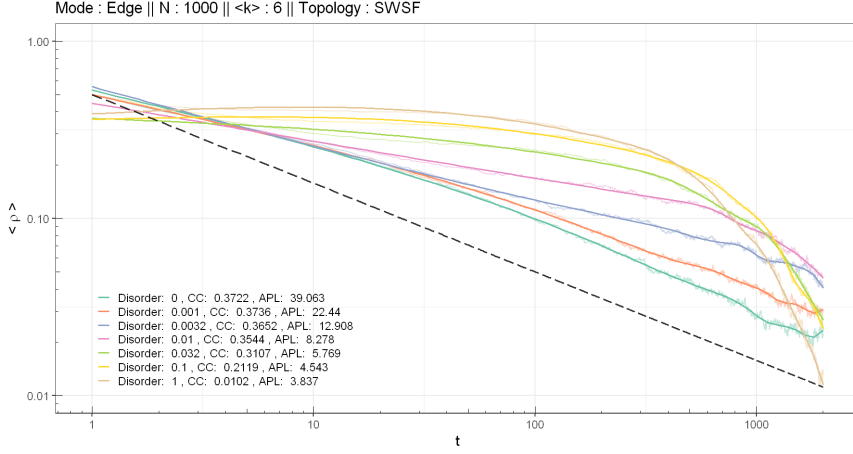


Figure 1.4: Variance of the average interface density for different values of disorder subject to the edge-update rule. averaged over 128 realizations.

same behavior  $\langle \rho \rangle = t^{-0.498}$  for the SW but the exponent for the SSF network is -0.46 which is higher than  $-1/2$ . This is a different behavior compared to the node-update rule while it could also be due to low number of nodes ( $N=2000$ ) or low number of realizations ( $= 32$ ).

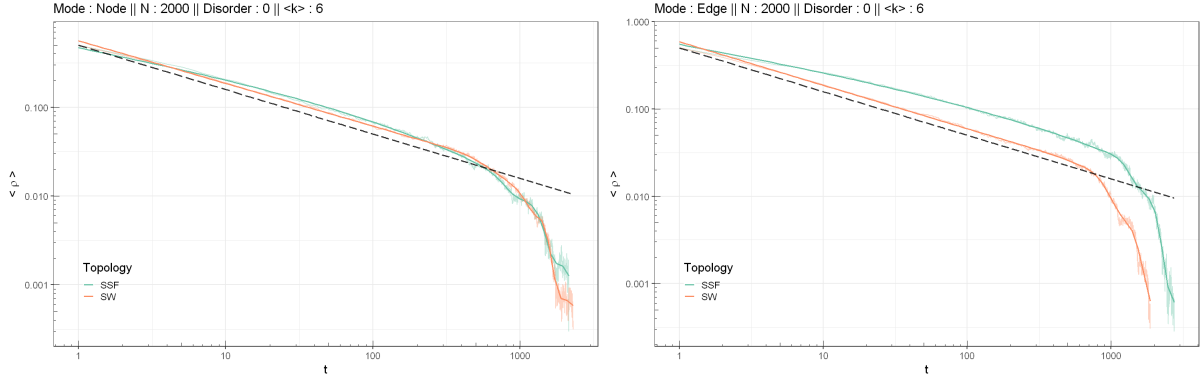


Figure 1.5: Effectively one dimensional networks subject to node and edge update rule. Dotted line refers to  $\langle \rho \rangle = 1/2t^{-1/2}$

On the opposite side of the spectrum, for  $p = 1$ , both RSF and RN show similar scaling with the number of nodes. The only notable difference between node-update and edge-update rule is the offset; in spite of the node-update, RSF and RN tend to converge to the absorbing state at similar rates (Fig. 1.6).

The plateau height shows no correlation with network size when updating the opinions based on nodes. Edge-update also shows no substantial dependence of  $\xi$  on  $N$  but the plateau value is strictly higher for SSF. However, the splitting is not large enough to suggest that edge-update can find a distinction based on the degree distribution while a more close comparison for varying  $\langle k \rangle$  shows more convincing results.

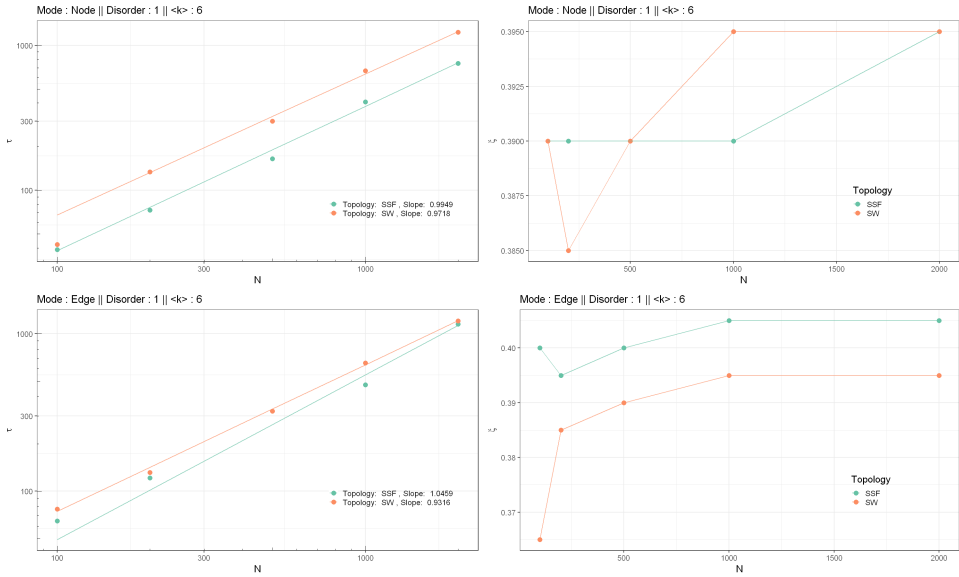


Figure 1.6: Lifetime and plateau with respect to network size over 64 realizations.

### 1.4.3 Node-update vs Edge-update

By varying the average degree of a network, we instinctively anticipate a significant impact on the evolution of the average interface density. Both plateau height and lifetime behave similarly for either edge or node update rules, while there is a clear and consistent gap between them. Therefore, while switching the update rule does not noticeably affect the behavior of  $\langle \rho \rangle$  with respect to  $\langle k \rangle$ , the gap previously seen in  $\xi$  and  $\tau$  via varying network size is confirmed Fig. 1.7.

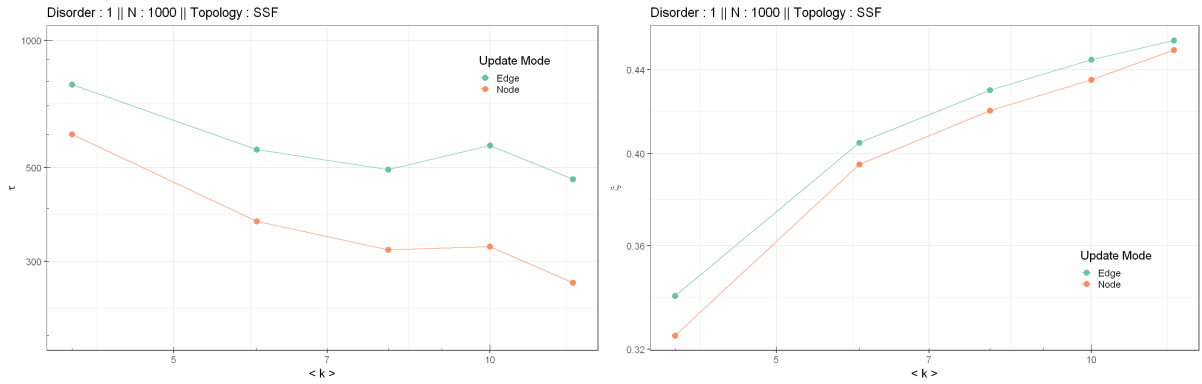


Figure 1.7: Plateau height and lifetime for RSF network against average degree. averaged over 32 realizations

## 2 | Axelrod model for dissemination of culture

---

**Task leader(s):** Davide Checchia, Giuseppe Bevilacqua

### 2.1 | Introduction

---

One of the most interesting and studied phenomena concerning human sociology is the emergence of diversity through the evolution of a system.

In this work we will focus on analyzing the emergence of cultural communities on two synthetic topologies by using Axelrod's Model for Dissemination of Culture [3]. We will then illustrate possible improvements and implementations with real world data.

### 2.2 | Model Description

---

We start by considering a regular  $L \times L$  lattice with  $N = L^2$  nodes. Each node is considered a **culture**  $c \in C$ , represented by a disordered tuple of  $F$  features ranging from 1 to  $q$ . Meaning that, for every  $c \in C : c = (f_1(c), f_2(c), \dots, f_F(c))$ ,  $f_i = \{1, 2, \dots, q\}$ .

Every feature is initialized **randomly**. After that, at each time step, we pick a node  $s$  at random and one of its  $R$ -order neighbors  $n_j$ . We calculate the probability of their interaction:

$$p(n_j \rightarrow s) = \frac{1}{F} \sum_{i=1}^F \delta(f_i(s) - f_i(n_j))$$

If the probability leads to a success (by uniform number draw) then a feature of  $s$  is chosen at random from the ones dissimilar to  $n_j$ , and is updated with the corresponding value from  $n_j$ , meaning  $f_k(s) \leftarrow f_k(n_j)$ . This counts as an **epoch**.

It is evident that a meaningful interaction only happens when  $0 < p < 1$ , as when  $p = 0$  the interaction cannot happen, while  $p = 1$  leads to no exchange of features.

This procedure is repeated until no interaction can happen. In this *frozen* state we can identify communities (nodes that share the exact same features) and their borders (since other neighboring communities will necessarily share no features).

This procedure is then extended to an Erdős–Rényi (ER) model (which is characterized by the number of nodes  $N$  and the average degree of the nodes  $\langle k \rangle$ ) and a synthetic model built on real-world data of Italian geography.

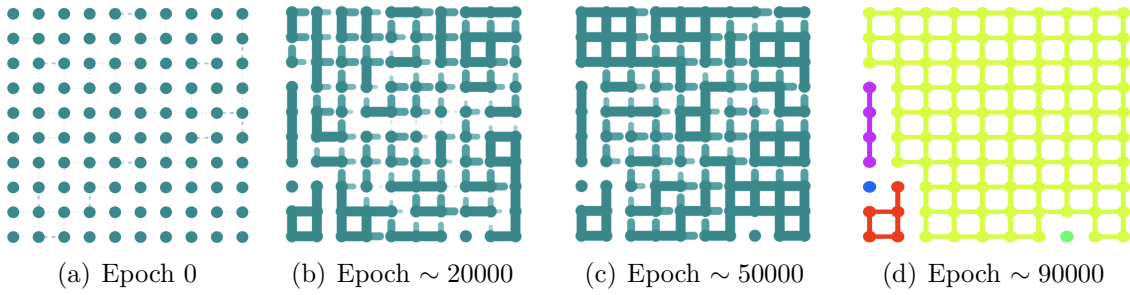


Figure 2.1: Example of evolution on Lattice model. The process is repeated until convergence (complete similarity or complete difference between nodes).

## 2.3 | Model Analysis

This section gives the methods and results for various change of parameters on both the Lattice and ER models.

We mainly study three parameters as succinct descriptors of our model, mainly:

- $n_c$ , the number of stable cultures in the frozen state,
- $\frac{S_{max}}{N}$ , the relative size of the largest stable community with respect to the number of nodes,
- $T_{co}$ , the number of epochs necessary for convergence.

### 2.3.1 Variation of $F$ and $q$

We first start our analysis by varying the number of features  $F$  and possible traits  $q$ , maintaining  $L$  (or  $N$ ,  $\langle k \rangle$  for ER) and  $R$  fixed.

By increasing the number of traits  $q$ , we observe a general increase in  $n_c$  for both models. This is expected, since by having more traits per feature, the chance of being similar goes down.

By increasing the number of traits  $F$ , we observe a decrease in  $n_c$  for the Lattice model, but not for ER. This could be explained by having more chance of similarity between nodes, and thus interaction. The results can be checked in table 2.1 and table 2.3.

### 2.3.2 Variation of $R$

By increasing the order  $R$  of neighboring, we observe a severe reduction in  $n_c$ . This is expected, as by increasing  $R$  from  $R = 1$  to  $R = 2$  we start considering the neighbors' neighbors for the interaction , see table 2.2.

### 2.3.3 Topological traits

We change, respectively,  $L$  for the Lattice model,  $N$  and  $\langle k \rangle$  for the ER model, and measure the number of communities  $n_c$ .

For the Lattice model, a weird behavior is observed: the number  $n_c$  increases up to a maximum around  $L = 10$  ( $n_c \approx 25$ ), then it decreases for larger and larger values

of  $L$  2.3(a). This is due to the fact that the dynamics of the boundary is that of the random-walk [3].

For the ER model, we measure the relative number of communities with respect to the size,  $\frac{n_c}{N}$ . We observe, for different value of  $N$ , a consistent decreasing behavior with respect to  $\langle k \rangle$ , suggesting a linear dependence  $n_c \sim O(N)$  2.3(e).

By measuring the time of convergence  $T_{co}$ , a polynomial relationship is observed with respect to  $L$  2.3(b), whereas we observe a plateau with respect to  $\langle k \rangle$  for ER 2.3(g).

| Number of cultural features ( $F$ ) | Number of traits per feature ( $q$ ) |      |       |
|-------------------------------------|--------------------------------------|------|-------|
|                                     | 5                                    | 10   | 15    |
| 5                                   | 1.05                                 | 3.91 | 20.22 |
| 10                                  | 1.00                                 | 1.06 | 1.48  |
| 15                                  | 1.00                                 | 1.00 | 1.09  |

Table 2.1: The table displays the average number of stable regions  $n_c$  for different values of  $F$  and  $q$ , while maintaining  $L = 10$  (Lattice model). The results are averaged across 32 runs.

| Number of cultural features ( $F$ ) | Number of traits per feature ( $q$ ) |      |      |
|-------------------------------------|--------------------------------------|------|------|
|                                     | 5                                    | 10   | 15   |
| 5                                   | 1.00                                 | 1.10 | 3.20 |
| 10                                  | 1.00                                 | 1.00 | 1.00 |
| 15                                  | 1.00                                 | 1.00 | 1.00 |

Table 2.2: The table displays the average number of stable regions  $n_c$  for different values of  $F$  and  $q$ , while maintaining  $L = 10$ ,  $R = 2$  (Lattice model). The results are averaged across 16 runs.

## 2.4 | Phase transition and active bonds

We observed the emergence of one big stable region ( $\frac{S_{max}}{N} \sim 1$ ) for low values of  $q$ , correlated to a low  $n_c$  value (and thus, a **mono-cultural system**) [10].

By increasing the number of traits we observe a **phase transition** towards a **multi-cultural system** ( $\frac{S_{max}}{N} \ll 1$ ). As such, we may expect a critical value  $q_c$  of transitioning. This is found for the Lattice model (at different  $L$ ) 2.3(c), whereas we do not necessarily observe a clean transition for the ER model (at different  $N$ ) 2.3(f).

By measuring the density of active bonds  $n_a$  (i.e. the fraction of edges that **allow** an interaction,  $p \neq 0$  and  $p \neq 1$ ) we observe an initial rise for values of  $q$  related to mono-cultural system, followed by a steady decrease [4]. For multi-cultural system this seems to fade (as  $q$  increases), allowing quick convergence to a frozen state. Results can be seen in 2.3(d).

| Number of cultural features ( $F$ ) | Number of traits per feature ( $q$ ) |      |      |
|-------------------------------------|--------------------------------------|------|------|
|                                     | 10                                   | 15   | 20   |
| 5                                   | 2.19                                 | 3.06 | 6.56 |
| 10                                  | 2.00                                 | 2.26 | 2.75 |
| 15                                  | 2.38                                 | 2.31 | 2.81 |

Table 2.3: The table displays the average number of stable regions  $n_c$  for different values of  $F$  and  $q$  and maintaining  $N = 200$  and  $\langle k \rangle = 5$  (ER Model). The results are averaged across 32 runs.

## 2.5 | Real-world data

In this section we suggest an implementation of a community-forming real world quantity: **elevation**.

This is based on the fact that, in theory, villages should communicate more if their altitude is similar, whereas difference in altitude (i.e. one village resides on a mountain, the other in a valley) should discourage interactions. We model that by defining a modified probability of interaction:

$$p(n_j \rightarrow a) = \left[ \frac{1}{F} \sum_{i=1}^F \delta(f_i(a) - f_i(n_j)) \right] \times \left[ (1-w) + w \frac{\zeta}{|z_a - z_{n_j}| + \zeta} \right]$$

Where  $w$  is a **weight-parameter**: when  $w = 0$  we get the classical probability, whereas  $w = 1$  leads to a product of the two probabilities.

The elevations are represented as  $z_a$  and  $z_{n_j}$ , whereas  $\zeta$  is a **normalization constant** defining how much to value the relative difference in heights.

We chose a list of Italian cities, each associated with latitude and longitude [6]. Via freely-available elevation database, using a python API, we retrieved the elevation for each city [1].

We then connected each node by evaluating the **Haversine distance** between them and setting a threshold of  $d = 150\text{km}$  (meaning that if the real-world distance between two nodes was less than the threshold, those were to be connected). The plotted graph can be shown in 2.2, and serves as a decent approximation for Italy. Further information characterizing the graph, as the degree-distribution, is shown in 2.3(j).

By varying  $F$  and  $q$  (but setting  $w = 0$ ), we observe shared behaviors with the ER model, as seen in 2.4. After picking a set of  $F$  and  $q$  values, we then focus on changing the values for  $w$  and  $\zeta$  (The effects of  $\zeta$  on the probability can be seen in 2.3(i)).

Against the initial assumption, no significant change of  $n_c$  nor  $\frac{S_{max}}{N}$  is observed (2.3(k), 2.3(l)), requiring more analysis on elevation, perhaps on a regular lattice (or a different formulation for the probability).

| Number of cultural features ( $F$ ) | Number of traits per feature ( $q$ ) |      |      |
|-------------------------------------|--------------------------------------|------|------|
|                                     | 15                                   | 20   | 25   |
| 10                                  | 3.00                                 | 4.88 | 5.88 |
| 15                                  | 2.38                                 | 2.25 | 3.25 |
| 20                                  | 2.13                                 | 2.13 | 2.50 |

Table 2.4: The table displays the average number of stable regions  $n_c$  for different values of  $F$  and  $q$ , given  $w = 0$  (Italy). The results are averaged across 16 runs.

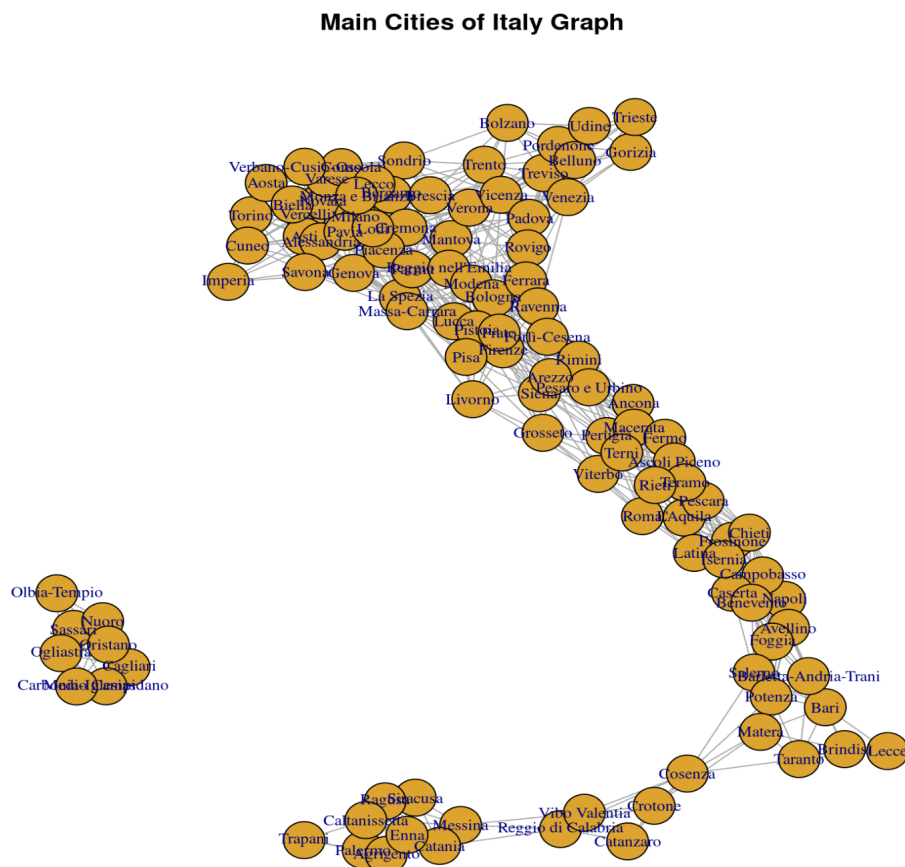
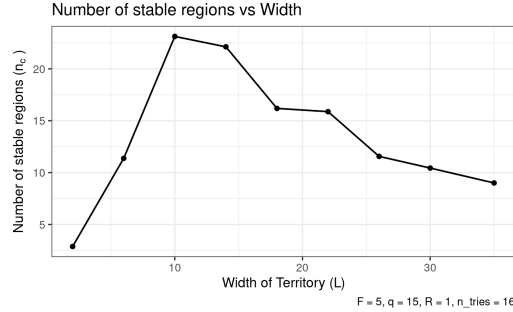
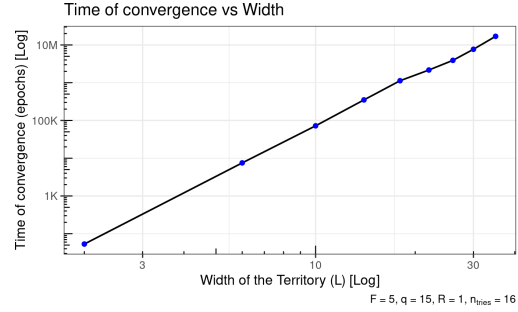


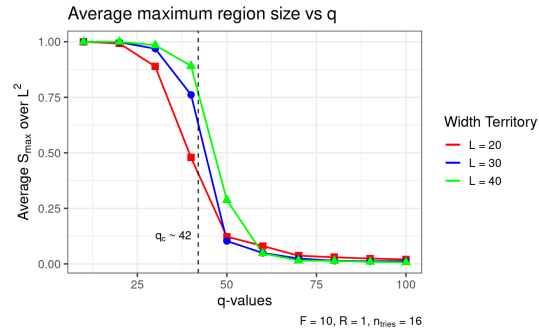
Figure 2.2: Graph of Italy, obtained via read of nodes list, after applying Haversine distance and threshold.



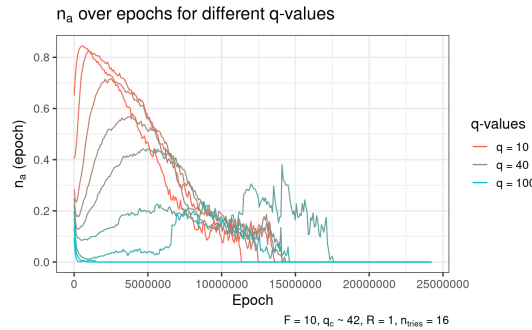
(a)  $n_c$  as a function of  $L$  (Lattice Model).  $F = 5, q = 15, R = 1, n_{tries} = 16$ .



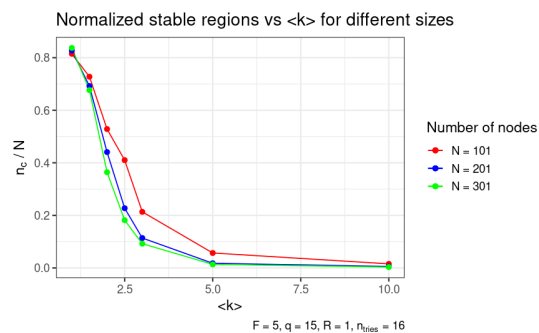
(b)  $T_{co}$  as a function of  $L$  (Lattice model, logarithmic scale).  $F = 5, q = 15, R = 1, n_{tries} = 16$ . Slope of the line is  $4.42 \pm 0.11$ .



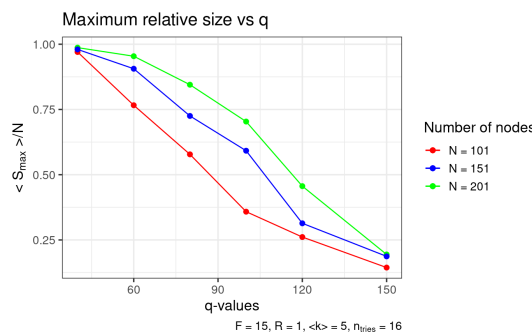
(c)  $\frac{S_{max}}{N}$  as a function of  $q$  (Lattice model).  $F = 10, R = 1, n_{tries} = 16$ .



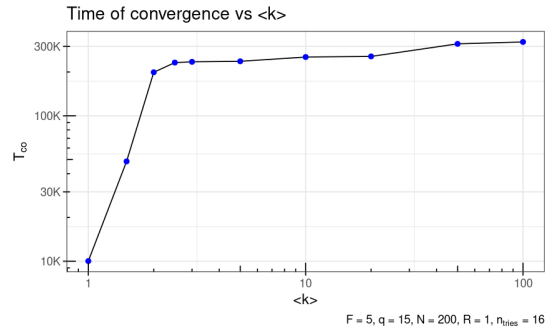
(d)  $n_\alpha$  as a function of  $t$  for  $q = 10, 20, 30, 35, 40, 45, 55, 70, 100$  ( $q_c \approx 42$ ) (Lattice model). Only the first, middle and last colours are noted: the rest follows the gradient proportionally to  $q$ .  $F = 10, R = 1, n_{tries} = 16$ .



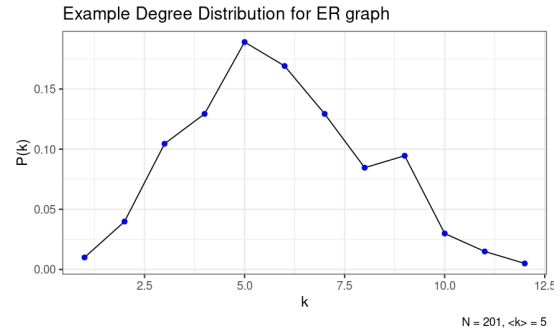
(e) Normalized number of stable regions  $\frac{n_c}{N}$  as a function of  $\langle k \rangle$  (ER model).  $F = 5, q = 15, R = 1, n_{tries} = 16$ .



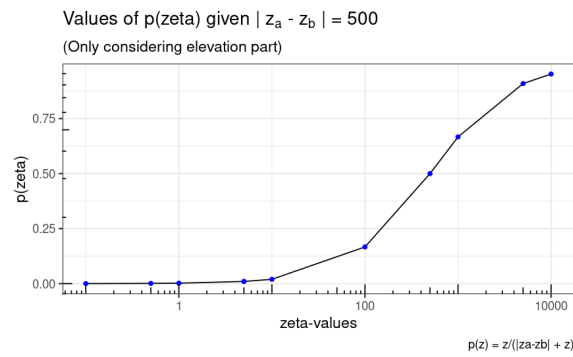
(f) Max stable region size  $\frac{S_{max}}{N}$  as a function of  $q$  (ER model).  $F = 15, R = 1, \langle k \rangle = 5, n_{tries} = 16$ .



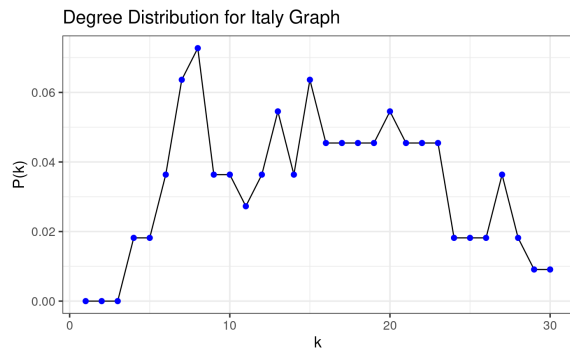
(g) Time of convergence  $T_{co}$  as a function of  $\langle k \rangle$  (ER model).



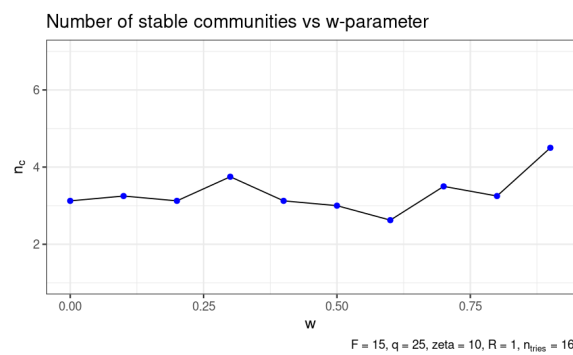
(h) Example of a Degree Distribution  $P(k)$  for ER model,  $N = 201, \langle k \rangle = 5$ .



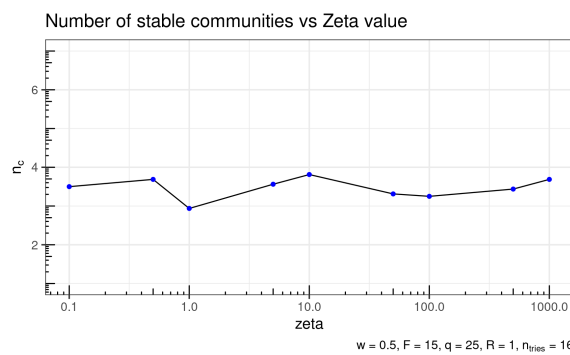
(i) How  $p(\zeta)$  behaves when fixing both classical compatibility and height difference.



(j) Degree Distribution  $P(k)$  for Italy Graph.



(k) Number of stable communities  $n_c$  as a function of the weight parameter  $w$ . Notice almost no relationship between the variables.



(l) Number of stable communities  $n_c$  as a function of the normalization constant  $\zeta$ . Notice almost no relationship between the variables.

# 3 | Language Competition Dynamics

---

**Task leader(s):** *Joan Verguizas I Moliner*

## 3.1 | Introduction

---

In today's interconnected world, languages find themselves without the natural or political borders that many years ago used to separate them. This phenomena has lead to the spread of languages beyond their places of origin giving birth to bilingual communities. In those communities, the coexistence of languages leads to a dynamic in which they compete for dominance in everyday communication.

In this work we will study the language competition dynamics that arises between languages in a bilingual community. In order to do that, we will simulate a competition between two languages and study how the outcome changes when varying different parameters as well as the topology of our model.

## 3.2 | Model Description

---

To simulate the language competition we will make use of a lattice-like structure with  $N = L \times L$  nodes where each node in the lattice is an agent (speaker) of the bilingual community. Each of the nodes are initialized at random with an uniform probability for the different speaking communities.

Once the initial state is established we will iterate by a number of  $N$  epochs the main algorithm. This will consist in picking a random node  $i$  from the lattice and after computing the local densities  $\sigma_i$  of each linguistic community in the neighbourhood of agent  $i$  we will be able to get the probabilities in which the agent  $i$  can change from one linguistic community to another one. Finally, by sampling a random number considering the before mentioned probabilities the linguistic community of the agent will be decided.

We can define two different models for performing this task: The Abrams-Strogatz model and the Bilingual model. Both of them are defined in [14].

The Abrams-Strogatz model supposes that the agents within our community can be in two states. We will call them language A and language B. Their corresponding transition probabilities of them are:

$$p_{i,A \rightarrow B} = \frac{1}{2}\sigma_i^B \quad p_{i,B \rightarrow A} = \frac{1}{2}\sigma_i^A$$

Where  $\sigma_i^A$  and  $\sigma_i^B$  corresponds to the local densities of language users of each linguistic community in the neighborhood of agent i.

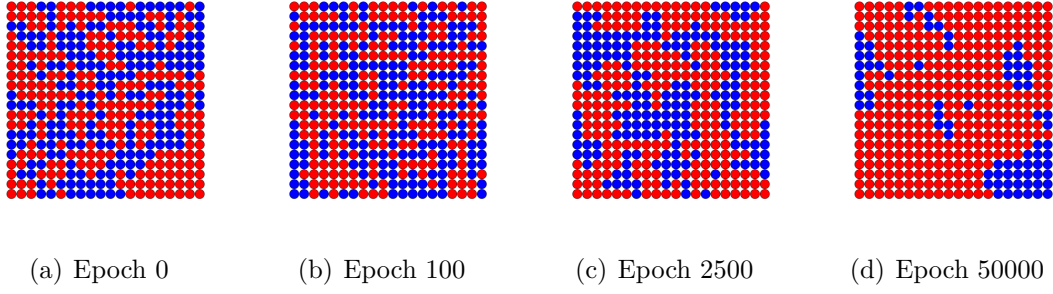


Figure 3.1: Example of the evolution of the language dynamics competition for the Abrams-Strogatz model.

On the other hand, the bilingual model supposes also the existence of bilingual agents within our community. We will call them AB. Now the transition probabilities of our agents will be:

$$\begin{aligned} p_{i,A \rightarrow AB} &= \frac{1}{2}\sigma_i^B & p_{i,B \rightarrow AB} &= \frac{1}{2}\sigma_i^A \\ p_{i,AB \rightarrow B} &= \frac{1}{2}(1 - \sigma_i^A) & p_{i,AB \rightarrow A} &= \frac{1}{2}(1 - \sigma_i^B) \end{aligned}$$

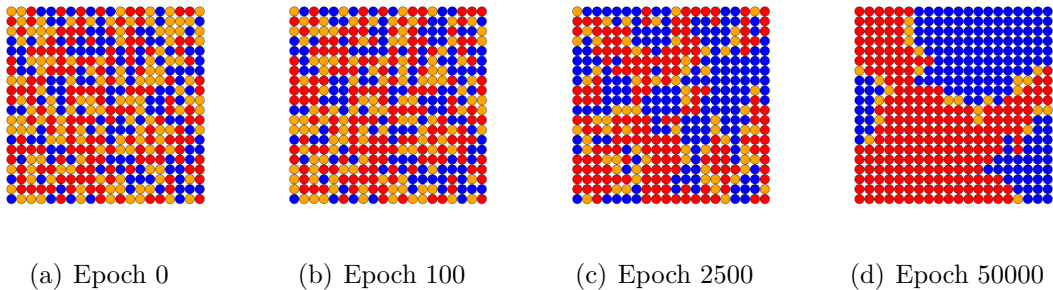


Figure 3.2: Example of the evolution of the language dynamics competition for the Bilingual model.

As observed in 3.1 and 3.2 as the number of epochs increase, spatial domains of each monolingual community are formed and grow in size. Bilingual communities are never formed instead they place themselves in a narrow band between the two monolingual domains.

### 3.3 | Model Analysis

In this section we are going to study both the Abrams-Strogatz and the Bilingual model changing some of the parameters used to characterize the network as well as changing the topology of how our network is created.

In order to study the outcome of these changes we are going to use the mean interface density  $\rho$ . This is defined as the density of links joining nodes in the network which are in different states. The minimum value  $\rho = 0$  corresponds to a stationary configuration in which all the agents belong to the same linguistic community.

### 3.3.1 Number of Nodes N

The first parameter that we can consider changing is the number of nodes  $N$  and see if by increasing the lattice size the number of epochs to get to extinction changes.

We can see that the average interface density decays as a power law:  $\langle \rho \rangle \sim t^{-\gamma}$  in both models 3.3 and the decay slows as we increase the number of nodes in our lattice. In both models the  $\gamma$  parameter gets lower as we increase the size of our network 3.5

### 3.3.2 Changing the Topology

In order to study the effects that the social structure has in the evolution of the models we make use of a small-world (also called Watts-Strogatz) topology instead of the lattice-like we have been using for now. This one introduces a rewiring probability  $p$ . Basically how likely is that one of the endpoints of an edge changes.

As we can see in 3.4, a small world topology in the bilingual model produces a fast extinction of one of the monolingual communities. Meanwhile, the effect of changing  $p$  is not very big in the Abrams-Strogatz model. We can see that when comparing the  $\gamma$  for different values of  $p$  in 3.4.

We can also introduce a community structure topology that consists of a combination of random attachment with a search for new contacts in the neighborhood of our random connections we have made. This process is repeated a number of times depending if we want to create more or less community structure. At 3.7 we can see the degree distribution depending on the number of iterations.

An extended explanation of this algorithm and its implementation can be found in [11].

When plotting the average interface density at 3.8 we can see that a community structure topology seems to make the model converge slower which correlates of what should we expect as it acts as resilient factor. In the Bilingual case though the model with more community structure converges faster which may be due to the fact that we are working with a network of  $N=100$  nodes and introducing a lot of connections in the network may instead make the community structure act as a global connected network at the limit.

### 3.3.3 Prestige and Volatility

Prestige and volatility can be used to model a change in the status of the two competing languages and a change in how fast agents take to imitate neighboring agents status respectively. We will model this for the Abrams-Strogatz model. The new transition probabilities will be:

$$p_{i,A \rightarrow B} = (1 - s)(\sigma_i^B)^a \quad p_{i,B \rightarrow A} = s(\sigma_i^A)^a$$

Where  $a$  represents volatility and  $s$  the prestige. At  $a > 1$  an agent is affected by local majorities changes below random imitation while for  $a < 1$  this probability will be above random imitation. Meanwhile, if  $s > 0.5$  there will be a preference for language A and for  $s < 0.5$  will be a preference for language B.

As expected as the prestige gets further from  $s = 0.5$  the number of epochs needed to get into the extinction state is lower. In the same way as we increase the volatility the convergence into a monolingual community is also faster [3.5](#).

### 3.4 | Modelling the Dynamics of Language Death

We can use the probability of transition that takes into account volatility and prestige in the Abrams-Strogatz model with real world data in order to model the dynamics of language death. The evolution dynamics is defined by the following ODE:

$$\frac{dx}{dy} = \sigma_B p_{B \rightarrow A} - \sigma_A p_{A \rightarrow B}$$

Where in this case we consider the densities  $\sigma_B$  and  $\sigma_A$  as the ones for the whole population. With this in mind we have fitted data that we gathered for different minority languages to this ODE in order to infer the parameters  $a$  and  $s$ . Being those Welsh in Wales [\[5\]](#), Irish in Ireland [\[7\]](#) and Gaelic Scottish in Sutherland, Scotland [\[13\]](#). This data can be referenced at [3.1](#), [3.2](#) and [3.3](#) respectively.

The result of fitting the data can be viewed at [3.6](#). In doing so we are able to infer the  $s$  and  $a$  parameters for each language, the results are shown at table [3.6](#).

The prestige value for the three languages falls inside the margin of error found at [\[2\]](#) of  $1.31 \pm 0.25$  with the exception of Gaelic Scottish that falls outside of it by a little bit.

On the other hand, when calculating the prestige we get approximately the same results as the paper. The computed prestige is 0.453 for Welsh and 0.296 for Gaelic Scottish while the paper gets 0.43 and 0.33 prestige values. The Irish language is not one of the languages studied in [\[2\]](#) so we can't compare its results.

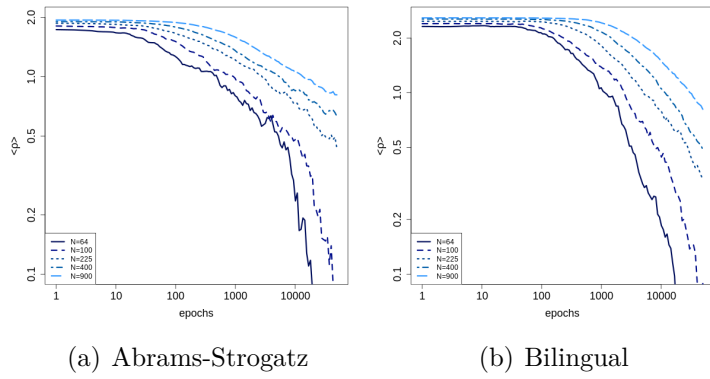


Figure 3.3: Evolution of the average interface density by different values of  $N$ . The results are averaged for 25 iterations.

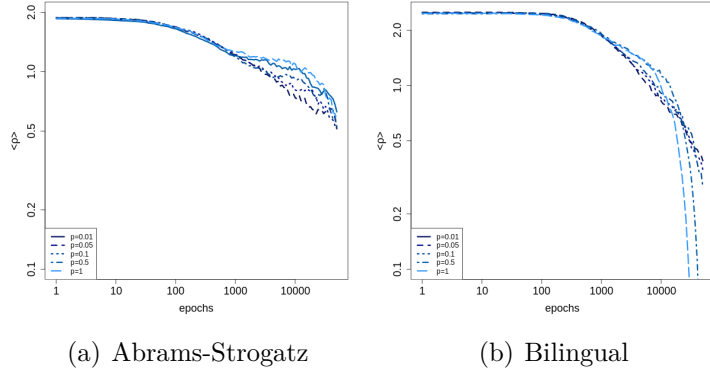


Figure 3.4: Evolution of the average interface density for a lattice structure with  $N=225$  and with different rewiring probabilities  $p$ . The results are averaged for 25 iterations.

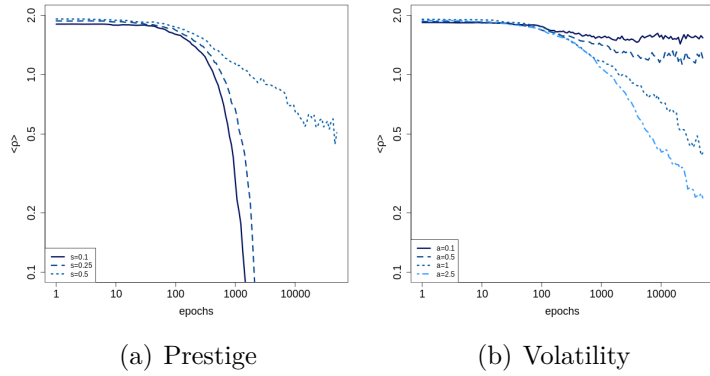


Figure 3.5: Evolution of the average interface density for a lattice structure with  $N=225$  with different values of volatility and prestige using the Abrams-Strogatz model. The results are averaged for 8 iterations.

| Year | Welsh Speakers |
|------|----------------|
| 1891 | 0.545          |
| 1901 | 0.499          |
| 1911 | 0.435          |
| 1921 | 0.371          |
| 1931 | 0.368          |
| 1951 | 0.289          |
| 1961 | 0.260          |
| 1971 | 0.209          |
| 1981 | 0.187          |
| 1991 | 0.186          |
| 2001 | 0.208          |
| 2011 | 0.190          |

Table 3.1: The table displays the evolution of the number of Welsh speakers in Wales.

| Year | Irish Speakers |
|------|----------------|
| 1821 | 0.550          |
| 1835 | 0.514          |
| 1841 | 0.506          |
| 1851 | 0.233          |
| 1861 | 0.191          |
| 1871 | 0.151          |
| 1891 | 0.145          |
| 1901 | 0.144          |
| 1911 | 0.133          |

Table 3.2: The table displays the evolution of the number of Irish speakers in Ireland (32 counties).

| Year | Gaelic Scottish Speakers |
|------|--------------------------|
| 1881 | 0.804                    |
| 1891 | 0.771                    |
| 1901 | 0.7175                   |
| 1911 | 0.618                    |
| 1921 | 0.523                    |
| 1931 | 0.441                    |
| 1951 | 0.253                    |
| 1961 | 0.188                    |
| 1971 | 0.145                    |

Table 3.3: The table displays the evolution of the number of Gaelic Scottish speakers in Sutherland, Scotland.

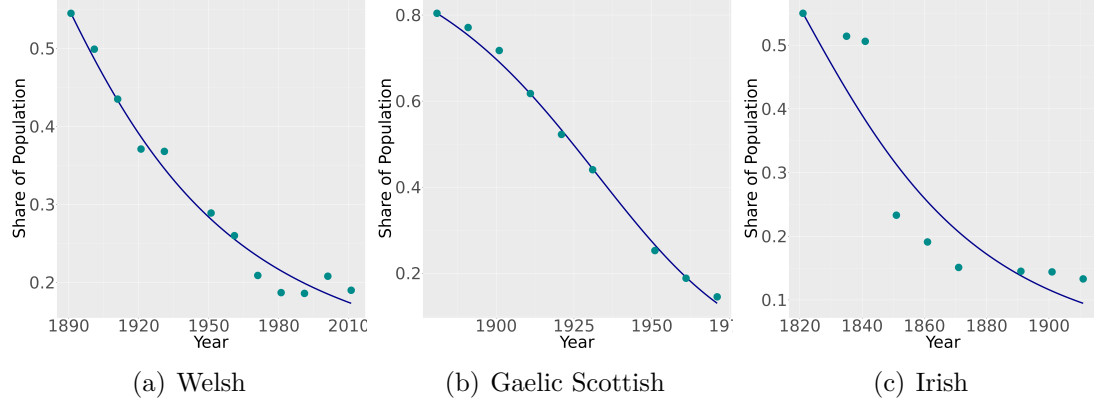


Figure 3.6: Evolution of the number of speakers of Welsh in Wales, Irish in Ireland and Gaelic Scottish in Sutherland, Scotland overtime.

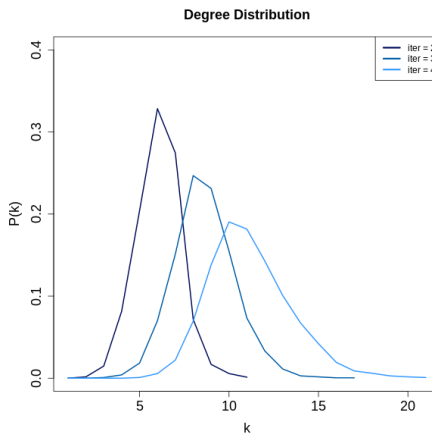


Figure 3.7: Degree distribution depending in the iterations used to generate the community structure topology for a lattice using 100 nodes. The result is averaged over 25 runs.

| Rewiring probability ( $p$ ) | $\gamma$ Parameter |           |
|------------------------------|--------------------|-----------|
|                              | Abrams-Strogatz    | Bilingual |
| 0.01                         | 0.136              | 0.182     |
| 0.05                         | 0.125              | 0.178     |
| 0.1                          | 0.118              | 0.175     |
| 0.5                          | 0.100              | 0.215     |
| 1                            | 0.097              | 0.301     |

Table 3.4: The table displays the value of the decay of the average interface density for different parameters of  $N$ .

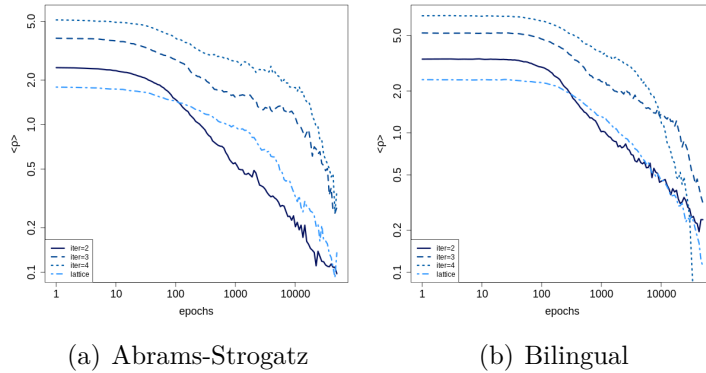


Figure 3.8: Average density interface evolution of different community structures for a network with  $N=100$ . The result is averaged over 25 runs.

| Number of Nodes ( $N$ ) | $\gamma$ Parameter |           |
|-------------------------|--------------------|-----------|
|                         | Abrams-Strogatz    | Bilingual |
| 64                      | 0.298              | 0.428     |
| 100                     | 0.260              | 0.305     |
| 225                     | 0.148              | 0.193     |
| 400                     | 0.123              | 0.152     |
| 900                     | 0.096              | 0.098     |

Table 3.5: The table displays the value of the decay of the average interface density for different parameters of  $N$ .

| Languages       | Parameters       |                    |
|-----------------|------------------|--------------------|
|                 | Prestige ( $s$ ) | Volatility ( $a$ ) |
| Welsh           | 0.453            | 1.245              |
| Irish           | 0.898            | 1.274              |
| Gaelic Scottish | 0.296            | 0.950              |

Table 3.6: The table displays the volatility and prestige of different languages after fitting the experimental data to the dynamics equation.

## 4 | Bibliography

---

- [1] Open-elevation api. <https://open-elevation.com/>. [Accessed 31-Aug-2023].
- [2] Daniel M. Abrams and Steven H. Strogatz. Modelling the dynamics of language death. *Nature*, 424(6951):900, August 2003. ISSN 1476-4687. doi: 10.1038/424900a. URL <https://doi.org/10.1038/424900a>.
- [3] Robert Axelrod. The dissemination of culture. *The Journal of Conflict Resolution*, 41(2):203–226, 1997.
- [4] Claudio Castellano, Matteo Marsili, and Alessandro Vespignani. Nonequilibrium phase transition in a model for social influence. *Phys. Rev. Lett.*, 85:3536–3539, 2000.
- [5] Janet Davies. *The Welsh Language, A History*. University of Wales Press, 2014.
- [6] Manlio De Domenico. Ita\_nodes.csv. List of nodes referring to main Italian cities, local file.
- [7] Reg Hingley. *The Death of the Irish Language*. Routledge, 1991.
- [8] Victor M. Eguiluz Konstantin Klemm. Highly clustered scale-free networks. *Phys. Rev. E*, 65(3):036123, 2002. doi: 10.1103/PhysRevE.65.036123. URL <https://arxiv.org/abs/cond-mat/0107606>.
- [9] Maxi San Miguel Krzysztof Suchecki, Víctor M. Eguíluz. Voter model dynamics in complex networks: Role of dimensionality, disorder and degree distribution. *Physical Review E*, 71:036132, 2005. URL <https://arxiv.org/abs/cond-mat/0504482>.
- [10] M.S. Miguel, V.M. Eguiluz, R. Toral, and K. Klemm. Binary and multivariate stochastic models of consensus formation. *Computing in Science & Engineering*, 7(6):67–73, 2005.
- [11] Jari Saramäki Jörkii Hyvönen Kimmo Kaski Riita Toivonen, Jukka-Pekka Onnela. A model for social networks. *Physica A: Statistical Mechanics and its Applications*, 371(2):851–860, 2006. ISSN 0378-4371. doi: <https://doi.org/10.1016/j.physa.2006.03.050>. URL <https://www.sciencedirect.com/science/article/pii/S0378437106003931>.

- [12] O. Shanker. Defining dimension of a complex network. *Modern Physics Letters B*, 21(06):321–326, 2007. doi: 10.1142/S0217984907012773. URL [https://www.researchgate.net/publication/243540799\\_Defining\\_Dimension\\_of\\_a\\_Complex\\_Network](https://www.researchgate.net/publication/243540799_Defining_Dimension_of_a_Complex_Network).
- [13] Charles W. J. Withers. *Gaelic in Scotland 1698–1981: The Geographical History of a Language*. John Donald, 1984.
- [14] Maxi San Miguel Lucía Loureiro-Porto Riita Toivonen J.Saramäki K. kaski Xavier Castelló, Víctor M. Eguíluz. Modelling language competition: Bilin-gualism and complex social networks. *The Evolution of Language: Proceedings of the 7th International Conference*, pages 59–66, 2008. doi: 10.1142/9789812776129\_0008. URL [https://www.worldscientific.com/doi/abs/10.1142/9789812776129\\_0008](https://www.worldscientific.com/doi/abs/10.1142/9789812776129_0008).